

DESCRIPTION OF THE SSB/A (SPECIAL SENSOR B/AEROSPACE)
X-RAY SPECTROMETER(U) AEROSPACE CORP EL SEGUNDO CA
SPACE SCIENCES LAB W A KOLASINSKI ET AL. 30 SEP 84
SD-TR-84-47 F04701-83-C-0084 F/G 22/2

NL

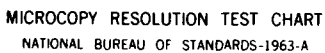
UNCLASSIFIED

F/G 22/2

END

FILMED

DTAC



MICROCOPY RESOLUTION TEST CHART
NATIONAL BUREAU OF STANDARDS-1963-A

12

Description of the SSB/A X-Ray Spectrometer

W. A. KOLASINSKI and P. F. MIZERA
✓Space Sciences Laboratory
Laboratory Operations
The Aerospace Corporation
El Segundo, Calif. 90245

AD-A150 040

30 September 1984

APPROVED FOR PUBLIC RELEASE;
DISTRIBUTION UNLIMITED

DTIC FILE COPY

DTIC
ELECTED
FEB 1 1985
S
A


Prepared for
SPACE DIVISION
AIR FORCE SYSTEMS COMMAND
Los Angeles Air Force Station
P.O. Box 92960, Worldway Postal Center
Los Angeles, California 90009

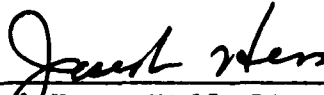
85 01 24 124

This report was submitted by The Aerospace Corporation, El Segundo, CA 90245, under Contract No. F04701-83-C-0084 with the Space Division, P.O. Box 92960, Worldway Postal Center, Los Angeles, CA 90009. It was reviewed and approved for The Aerospace Corporation by H. R. Rugge, Director, Space Sciences Laboratory. Lt. Col. John Bohlson, SD/YDA, was the project officer for the Air Force.

This report has been reviewed by the Public Affairs Office (PAS) and is releasable to the National Technical Information Service (NTIS). At NTIS, it will be available to the general public, including foreign nationals.

This technical report has been reviewed and is approved for publication. Publication of this report does not constitute Air Force approval of the report's findings or conclusions. It is published only for the exchange and stimulation of ideas.


John Bohlson, Lt Col, USAF
Project Officer


Joseph Hess, GM-15, Director, West Coast
Office, AF Space Technology Center

UNCLASSIFIED

SECURITY CLASSIFICATION OF THIS PAGE (When Data Entered)

REPORT DOCUMENTATION PAGE		READ INSTRUCTIONS BEFORE COMPLETING FORM	
1. REPORT NUMBER SD-TR-84-47	2. GOVT ACCESSION NO. A150040	3. RECIPIENT'S CATALOG NUMBER	
4. TITLE (and Subtitle) DESCRIPTION OF THE SSB/A X-RAY SPECTROMETER		5. TYPE OF REPORT & PERIOD COVERED	
7. AUTHOR(s) Wojciech A. Kolasinski and Paul F. Mizera		6. PERFORMING ORG. REPORT NUMBER TR-0084(4940-06)-1	
9. PERFORMING ORGANIZATION NAME AND ADDRESS The Aerospace Corporation El Segundo, Calif. 90245		8. CONTRACT OR GRANT NUMBER(s) F04701-83-C-0084	
11. CONTROLLING OFFICE NAME AND ADDRESS Space Division Los Angeles Air Force Station Los Angeles, Calif. 90009		10. PROGRAM ELEMENT, PROJECT, TASK AREA & WORK UNIT NUMBERS	
14. MONITORING AGENCY NAME & ADDRESS (if different from Controlling Office)		12. REPORT DATE 30 September 1984	
		13. NUMBER OF PAGES 40	
		15. SECURITY CLASS. (of this report) Unclassified	
		15a. DECLASSIFICATION/DOWNGRADING SCHEDULE	
16. DISTRIBUTION STATEMENT (of this Report) Approved for public release; distribution unlimited			
17. DISTRIBUTION STATEMENT (of the abstract entered in Block 20, if different from Report)			
18. SUPPLEMENTARY NOTES			
19. KEY WORDS (Continue on reverse side if necessary and identify by block number) Aurora, Ionospheric monitor, Remote sensing.			
20. ABSTRACT (Continue on reverse side if necessary and identify by block number) In this report we describe a scanning x- and gamma-ray spectrometer designed and built at The Aerospace Corporation's Space Sciences Laboratory for the Air Force Technical Applications Center (AFTAC). Designated as Special Sensor B/Aerospace (SSB/A), the instrument is on the Flight 6 Spacecraft of the Defense Meteorological Satellite Program (DMSP). The sensor is designed to locate and image atmospheric x-ray sources while providing data on their intensity as a function of energy in the 2-to-100-keV energy range. A small hydrogen Lyman-alpha emission detector has been placed on one of the two.			

DD FORM 1473
(FACSIMILE)

UNCLASSIFIED

SECURITY CLASSIFICATION OF THIS PAGE (When Data Entered)

UNCLASSIFIED

SECURITY CLASSIFICATION OF THIS PAGE(When Data Entered)

19. KEY WORDS (Continued)

20. ABSTRACT (Continued)

scanning heads so as to provide data coverage simultaneously with the x-ray measurements. Two Geiger-Mueller counters have also been mounted on the stationary platform of the spectrometer to provide measurements of electron fluxes for estimating local background in the x-ray measurements. Origin for

that the keywords include:

1. x-ray

UNCLASSIFIED

SECURITY CLASSIFICATION OF THIS PAGE(When Data Entered)

PREFACE

Special recognition is due to the following individuals for their efforts associated with designing the sensor, coordinating the project's development, and writing this report: W. T. Chater, C. K. Howey, S. S. Imamoto, N. Katz, C. G. King, P. H. Metzger, E. R. Schnauss, and R. L. Williams.

We are also grateful to W. R. Brooks, Sr., P. A. Carranza, M. K. Higashi, D. T. Katsuda, G. Roberts, D. Y. Watanabe, and W. J. Wong for working diligently to meet various production schedules. Finally, we thank J. Guines and his staff at the X-Ray Calibration and Standards Laboratory of Lawrence Livermore National Laboratory (LLNL) for making that facility available to us and providing support during SSB/A calibrations.

We also wish to acknowledge the continued support of the USAF Technical Applications Center, especially that from John Shrum.

A-1

Accusation For	
NITRO GRA&I	<input checked="" type="checkbox"/>
TAP	<input type="checkbox"/>
Handwritten	<input type="checkbox"/>
Classification	
Location/	
Activity Codes	
End/or	
Initial	



CONTENTS

PREFACE.....	1
I. INTRODUCTION.....	7
II. SENSOR CONFIGURATION AND CAPABILITIES.....	9
III. SENSOR-COMPONENT DESCRIPTION.....	17
A. High-Energy X-Ray Sensor (HEXS).....	17
B. Low-Energy X-Ray Sensor (LEXS).....	20
C. Geiger-Mueller Background Monitors (GMBM).....	22
D. Hydrogen Lyman-Alpha Radiation Monitor (HLARM).....	24
E. Scanner Drive and Control System.....	26
F. Data Processing System.....	27
IV. DATA FORMATS.....	33
A. Data Organization.....	33
B. Data Compression Scheme.....	39
REFERENCES.....	41
APPENDIX A. CONVERSION OF THE AEST WORDS FROM ANALOG (0 - 4.89 V) TO TEMPERATURE IN °C.....	43
APPENDIX B. CONVERSION OF INTERNAL SUBCOM VALUES FROM DIGITAL (OCTAL) TO TEMPERATURE IN °C.....	45
APPENDIX C. CONVERSION OF INTERNAL SUBCOM VALUES FROM DIGITAL (OCTAL) TO VOLTS.....	47

FIGURES

1.	Photograph of the SSB/A Instrument with the Front and Rear Thermal Covers Removed.....	10
2a.	Functional Block Diagram of the SSB/A Instrument.....	11
2b.	Detailed Electrical Block Diagram of the SSB/A Instrument.....	12
3.	Pictorial Representation of the SSB/A Instrument in Orbit, with the Spacecraft Axes Indicated.....	14
4.	Block Diagram of the High-Energy X-Ray Sensor (HEXS).....	18
5.	Block Diagram of the Low-Energy X-Ray Sensor (LEXS).....	21
6.	Block Diagram of the Geiger-Mueller (GM) Sensors.....	23
7.	Block Diagram of the Hydrogen Lyman-Alpha Radiation Monitor (HLARM).....	25

TABLES

1.	SSB/A Instrument Capabilities.....	13
2.	Scanner Pointing Directions.....	28
3.	Command Status Table.....	30
4.	SSB/A Data-Channel Organization.....	34
5.	List of Subcom Measurements.....	36
6.	Diagnostic Data (Group 1) Organization.....	37

I. INTRODUCTION

The Special Sensor B/Aerospace (SSB/A), described in this report, represents the third generation of remote x- and gamma-ray sensors developed at the Space Sciences Laboratory of The Aerospace Corporation for the Air Force Technical Applications Center (AFTAC). Originally the effort began with two "piggy-back" experiments (PBE's) flown successfully on Defense Meteorological Satellite Program (DMSP) Block 5C(F33) and Block 5D-1(F1) satellites as part of the GFE-4E sensor (B-package) built by Sandia National Laboratory. A more sophisticated sensor was subsequently developed for flight on the DMSP F2 and F5 spacecraft. These, named the "B-OMNI" sensors, were mounted on the spacecraft in a place previously reserved for another sensor known simply as the "GFE-6" and have therefore inherited that name. A detailed description of the GFE-6 is given in Ref. 1. The payload that flew on the DMSP F2 spacecraft performed extremely well and provided more than 2 years' worth of data. An analysis of some of that data appears in Ref. 2. Unfortunately, the second unit was launched on the ill-fated DMSP F5 spacecraft and now rests in Davy Jones' Locker.

Even before the GFE-6 sensors were launched, data from the second PBE aboard the F1 spacecraft prompted the development of the SSB/A. As a result of a malfunction in the attitude control system, the F1 spacecraft initially spun up and continued to spin for several months. The spin-modulated PBE data dramatically illustrated the advantages of a scanning sensor in the context of its ability to differentiate between background signals and those of interest.

Besides locating and identifying x-ray sources, the SSB/A data have proven very useful in studying the ionosphere, particularly in the auroral regions of the earth. For example, work currently in progress shows that absolute intensities and energy spectra of precipitating auroral electrons can be deduced from the SSB/A data (Ref. 3). Unlike particle detectors, which measure the flux only in the vicinity of the spacecraft, the SSB/A has a remote-sensing capability over wide regions on either side of the satellite ground track. Such image data are needed in the study of auroral processes. Furthermore, the data can be converted into energy-deposition profiles in the D and E regions of the ionosphere, and into electron density profiles and conductivity maps.

II. SENSOR CONFIGURATION AND CAPABILITIES

Figure 1 is a photograph of the SSB/A showing the physical configuration of the various components. For clarity, the side covers used for passive thermal control in orbit are shown detached from the instrument body. The whole instrument weighs 14.5 kg and consumes 9 W of power when all the components are operating. Figure 2 shows functional and electrical block diagrams of the SSB/A, illustrating in detail the major sensor subsystems and depicting the information flow. A detailed description of the individual components is provided in the next section, while the measurement capabilities of the detector subsystems aboard the SSB/A are summarized in Table 1. Figure 3 depicts in pictorial form the various measurements performed by the SSB/A, together with the visual data provided by the DMSP operational linescan system (OLS). Also defined in Fig. 3 are the spacecraft axes (x,y,z) to which we refer later in this report.

The two scanning heads are the unique feature of the SSB/A. They scan in opposition across a 110° arc that is perpendicular to the orbital plane and approximately centered about the subsatellite (nadir) point. One of the two heads carries the high-energy x-ray sensor (HEXS), which consists of three identical cadmium telluride (CdTe) detectors, each having a conical field of view with a 15° full angle. The HEXS spans an energy range between 15 keV and 100 keV in three differential channels and has an integral channel with a 100-keV energy threshold.

Coverage of the lower portion of the x-ray spectrum (>2 keV) is provided by the low-energy x-ray sensor (LEXS) in the form of a proportional counter mounted on the second scanning head. The LEXS has a rectangular field of view spanning full angles of 10° in-track and 20° cross-track. Appended to the LEXS head is a hydrogen Lyman-alpha emission detector, whose primary function is to monitor the photon flux emanating from precipitating protons.



SPACE RADIATION DETECTOR
SSB/A SCANNING X-RAY SPECTROMETER



Fig. 1. Photograph of the SSB/A Instrument with the Front and Rear Thermal Covers Removed. The main components are labeled.

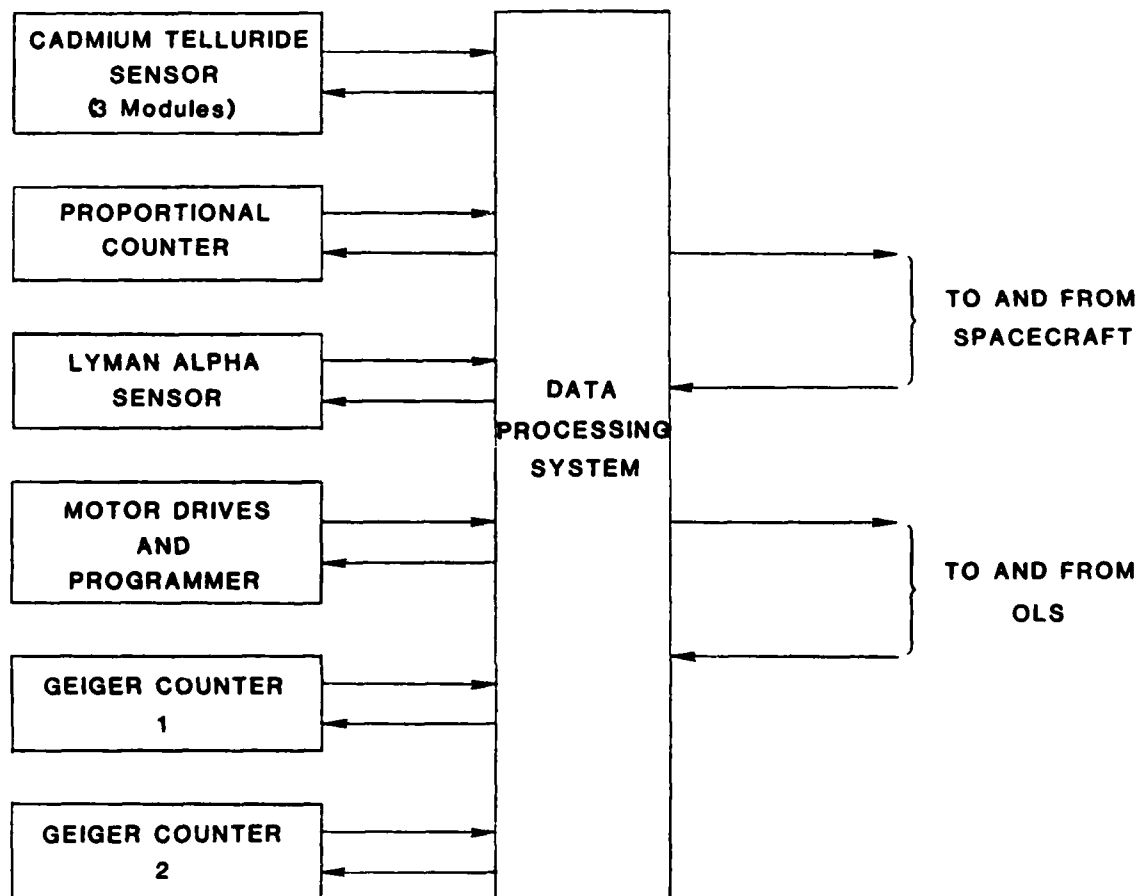


Fig. 2a. Functional Block Diagram of the SSB/A Instrument

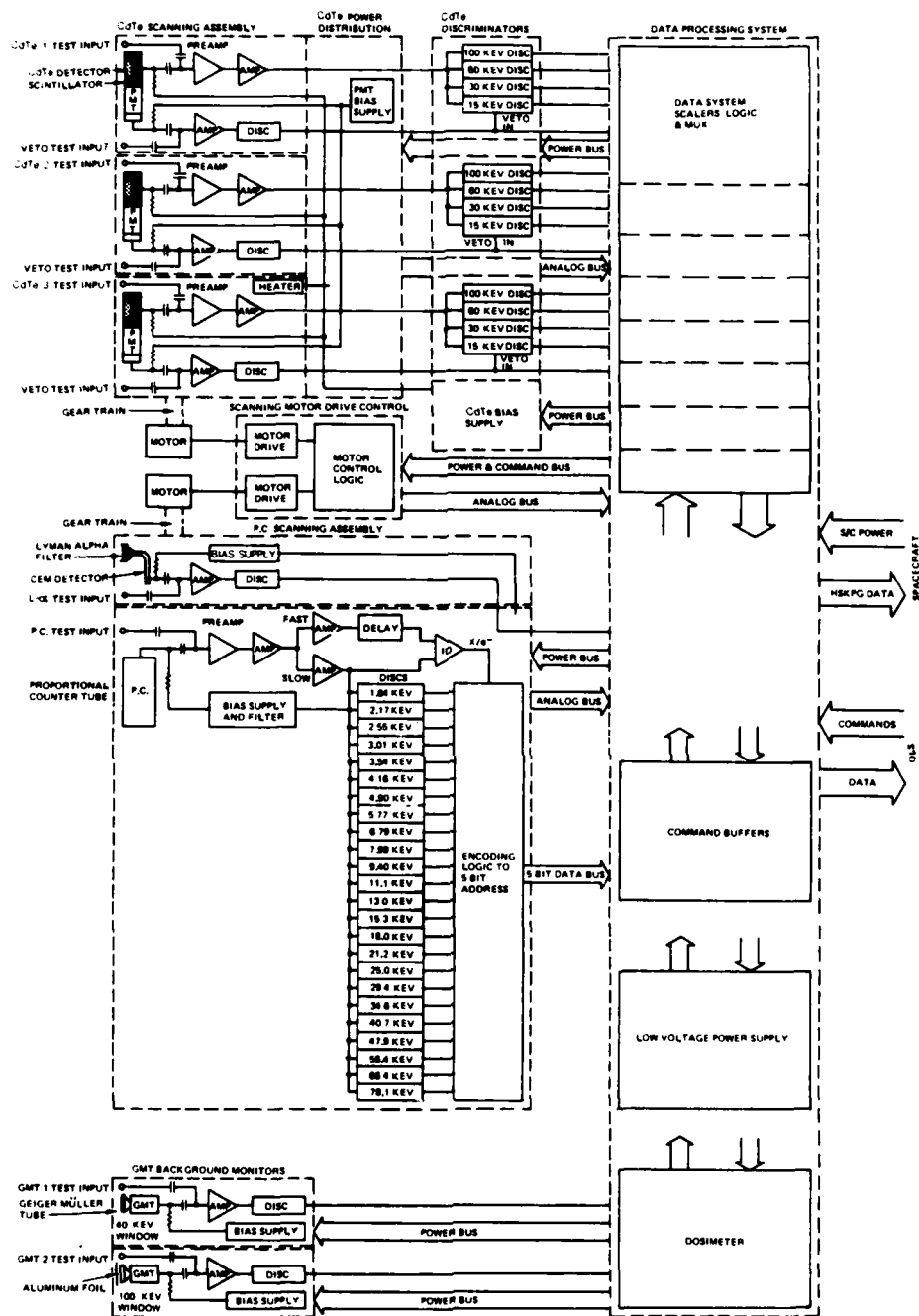


Fig. 2b. Detailed Electrical Block Diagram of the SSB/A Instrument

Table 1. SSB/A Instrument Capabilities

Instrument	Description	Measurements	Energy	Field of View	Look Direction
1) High-Energy X-Ray Sensor	Scanning CT detectors with anti-coincidence channeltron detectors	3 units	>15, 30, 60, 100 keV	7°.7°	x-y • x-z
2) Low-Energy X-Ray Sensor	Scanning proportional counter detectors with fast rise-time discrimination	24 (x rays) 6 (Bkg)	2 to 78 keV	5°.10°	x-y • x-z
3) Hydrogen Lyman-Alpha Radiation Monitor	Scanning Lyman-alpha filter with channeltron detector	1 channel	1216 Å	8°.14°	x-y • x-z
4) Geiger-Mueller Background Monitor	Stationary energetic electron monitors	2 units	>50 keV >100 keV	90°	y

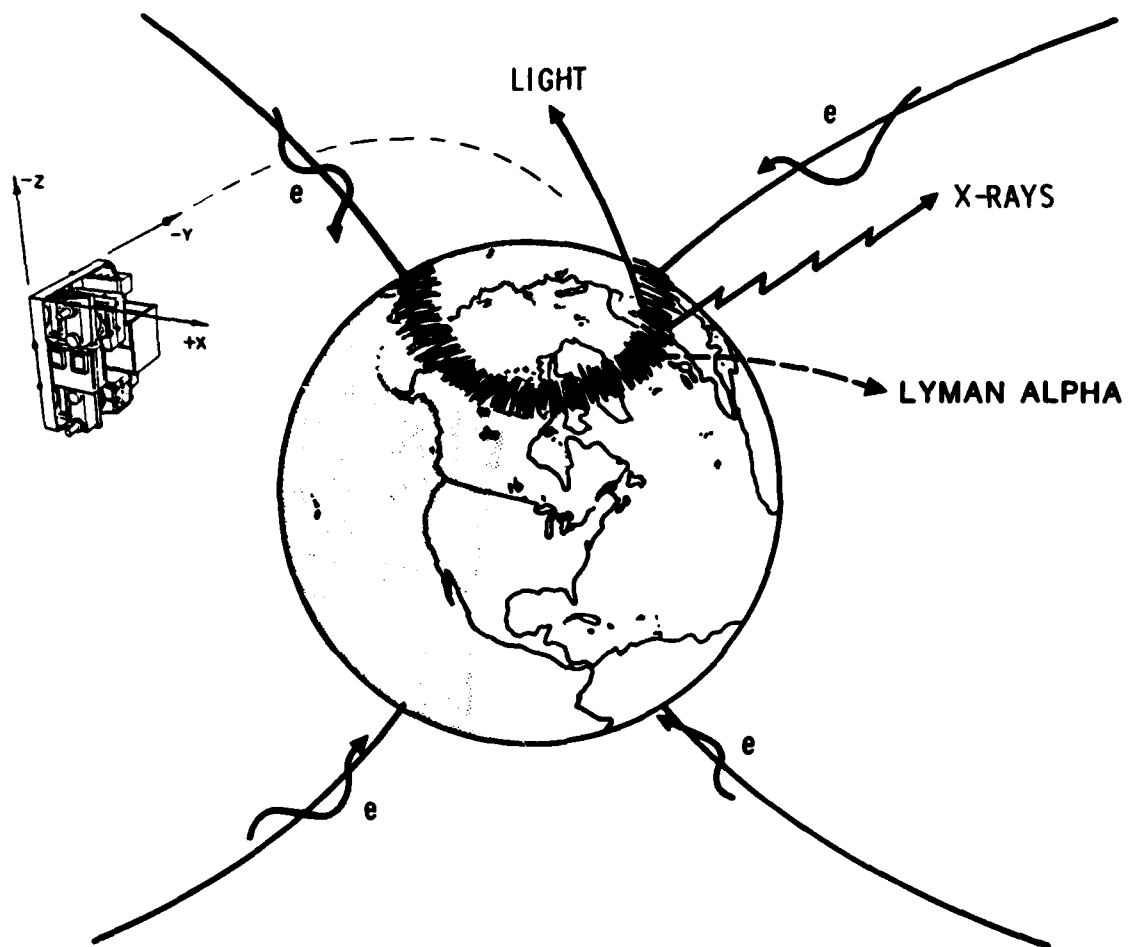


Fig. 3. Pictorial Representation of the SSB/A Instrument in Orbit, with the Spacecraft Axes Indicated. The northern lights are schematically shown, as well as hydrogen Lyman-alpha emissions and bremsstrahlung x rays.

In addition to the detector complement described above, two Geiger-Mueller (GM) counters have been placed on the fixed SSB/A platform as is shown in Fig. 1. Their purpose is to measure the integral flux of locally mirroring electrons having energies above ≈ 50 and ≈ 100 keV. These electrons, when striking the various structures near the x-ray detectors, generate x-rays by the bremsstrahlung process which can contaminate measurements of the atmospheric x-ray flux. Data from the GM counters will be used to estimate the severity of the background.

III. SENSOR-COMPONENT DESCRIPTION

A breakdown of the SSB/A into its major components appears in Fig. 2a in the form of a functional block diagram. This section gives a description of each of the component subsystems in sufficient detail to provide the reader with a basic understanding of each sensor's operation.

A. HIGH-ENERGY X-RAY SENSOR (HEXS)

A block diagram of the HEXS is shown in Fig. 4. It consists of three CdTe semiconductor (CT) detectors and their associated electronic circuits, with each detector being operated in a completely independent fashion. Each CT detector is approximately 1 cm^2 in area by 0.2 cm thick and is biased at approximately -610 V. The detectors have been individually potted in brass cups by means of Dow Corning 3110 RTV encapsulant. Subsequently, the cups have been covered with a beryllium entrance window 0.025 cm thick, and electrical connection to the detector has been made via coaxial cable, in order to minimize electrical and acoustical noise pickup. The detector assembly described above has in turn been encased in a NE-102 scintillator cup that is optically coupled to two EMR 521N-01-CM channel-electron photomultiplier tubes (PMTs) operated at $\sim +2800 \text{ V}$ bias. Signals from these PMTs, together with the respective CT detector signals, are applied to anticoincidence (veto) circuits that are used to prevent the counting of signals produced by penetrating charged particles. The CT detectors are collimated to a 15° conical viewing full-angle.

The CT detector analog signals, after proper amplification and shaping, are routed from the scanning head, through the hub, to three corresponding pulse-height analyzers (PHAs) on the stationary platform. Each PHA has three differential channels whose discriminator thresholds are set at 15, 30, and 60 keV, and one integral channel whose discriminator threshold is set at 100 keV. Analog signals from the PMTs are applied to the inputs of integral discriminators on board the scanning head and converted to logic pulses. The latter are also brought out through the hub and used to veto the PHA discriminator outputs.

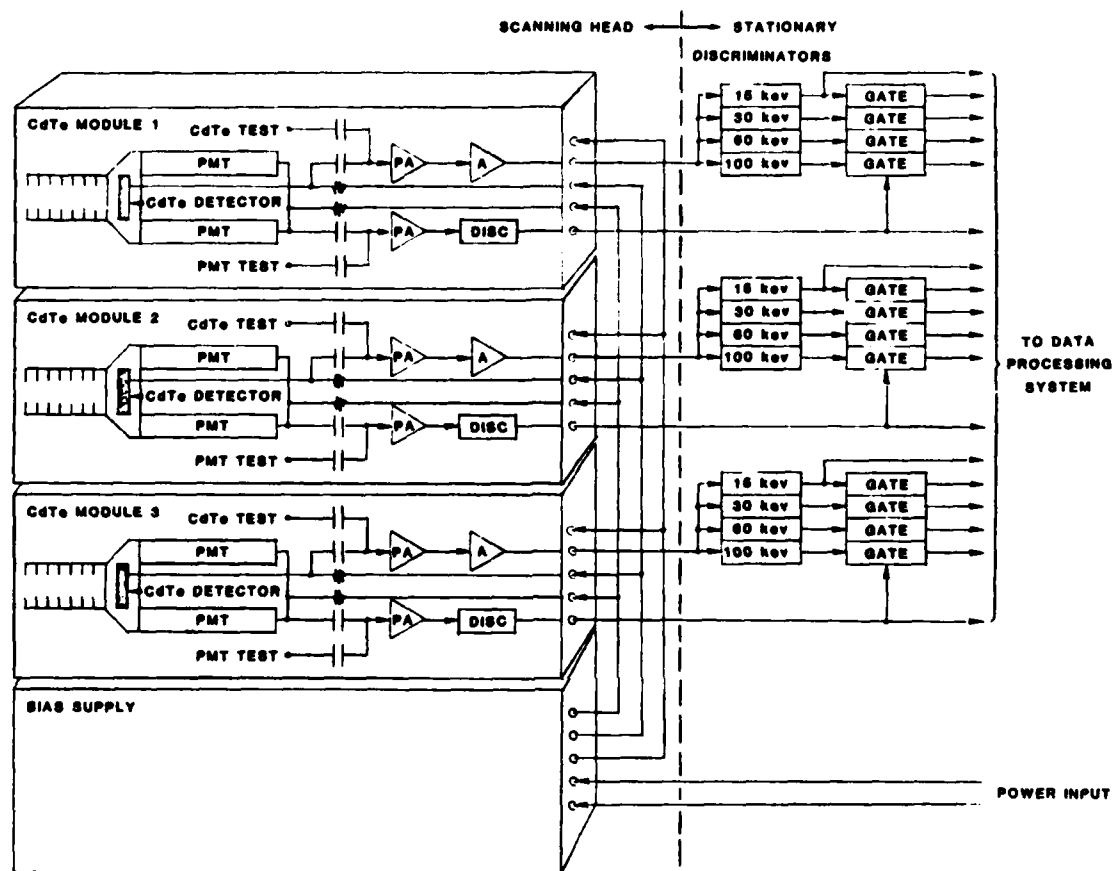


Fig. 4. Block Diagram of the High-Energy X-Ray Sensor (HEXS)

All output signals from the CT discriminator box are routed by means of coaxial cables to the data processing system (DPS) for counting and formatting into the data stream. There are six data outputs from each of the three CT detector systems: the four gated PHA outputs, an ungated integral output from the 15-keV discriminator, and the output of the veto discriminator. Hence there are 18 HEXS data channels in all.

The triple CT-detector scanning array also has a distribution board from which all power and signals are routed to and from the scanning head. The board includes monitors, fuses, and a bias supply for the PMTs, as well as a 1-W heater that turns on automatically at -18°C and off at -14°C . This heater has been added to protect the CT detectors from damage resulting from thermal stress at unduly cold temperatures that may occur when sensor power is off for a sufficiently long time. Under ordinary conditions the HEXS scanning head is passively constrained to maintain a temperature between 0 and -20°C , a range that is optimum for operating the CT detectors.

In operation, an x ray entering the CdTe crystal may be totally absorbed by an atom in the crystal lattice (the photoelectric effect) or scattered from one of the atomic electrons (Compton scattering). In either case, an energetic electron is ejected from the atom. This electron loses its energy by producing electron-hole pairs that are swept out by the applied electric field. The resulting pulse of charge at the detector electrodes is amplified by the charge-sensitive preamplifier (PA), properly shaped and further amplified by the shaping amplifier (A), and presented to the inputs of the PHA discriminators. Since the pulse height at the discriminator input is directly proportional to the total energy deposited in the crystal, a rough x-ray spectrum can be deduced from counting rates observed from the discriminator channels. Information concerning the location of the x-ray source can be obtained during the scanning mode by noting the scanner-head angle and satellite position when maximum intensity is measured.

Background pulses in the various detector channels can be generated by charged particles (e.g., cosmic rays) having sufficient energy to penetrate passive shielding around the CdTe crystals. In order to reduce this background, active anticoincidence shields have been placed around the crystals. A particle passing through the scintillating plastic causes the latter to emit light that in turn produces a signal at the photomultiplier tube anode. This signal triggers a low-level discriminator that produces a logic pulse used to veto the CT discriminator outputs. Thus, in principle, only x rays that enter the crystal without interacting in the surrounding plastic are counted by the gated PHA outputs. Since in the HEXS energy range the probability of an x-ray interaction in the plastic scintillator is small, a negligible number of x-ray events is eliminated by the veto system.

B. LOW-ENERGY X-RAY SENSOR (LEXS)

The low-energy x-ray sensor consists of a proportional counter (PC) and its associated electronics, shown schematically in Fig. 5. Basically the PC is a gas-filled square aluminum tube with four adjacent 0.01-cm-thick beryllium windows in one of its rectangular sides. The total window area is 3.7 cm^2 . A very thin, bare wire, insulated from the structure, runs through the middle of the tube and is biased at $\sim +2700 \text{ V}$. The tube is filled to a pressure of 3 atm with equal amounts of argon (Ar) and xenon (Xe) and a 10% admixture of CO_2 for quenching. An x ray passing through the gas gives up its energy to a photoelectron that, after traversing a short distance, loses its energy by ionizing a large number of gas atoms. The primary electrons that result from this ionization process are accelerated towards the positively biased wire, and after gaining sufficient energy they in turn knock out more electrons from gas atoms encountered along the way. Very near the wire, where the electric field is strongest, a large amount of secondary ionization is produced. This secondary ionization is proportional to the amount of primary ionization, and hence to the x-ray energy. After proper amplification and shaping, the pulse is presented to the input of a 24-channel differential pulse-height analyzer (PHA) whose outputs are gated, encoded, and routed to the data processing system (DPS) for counting and incorporation in the telemetry data stream.

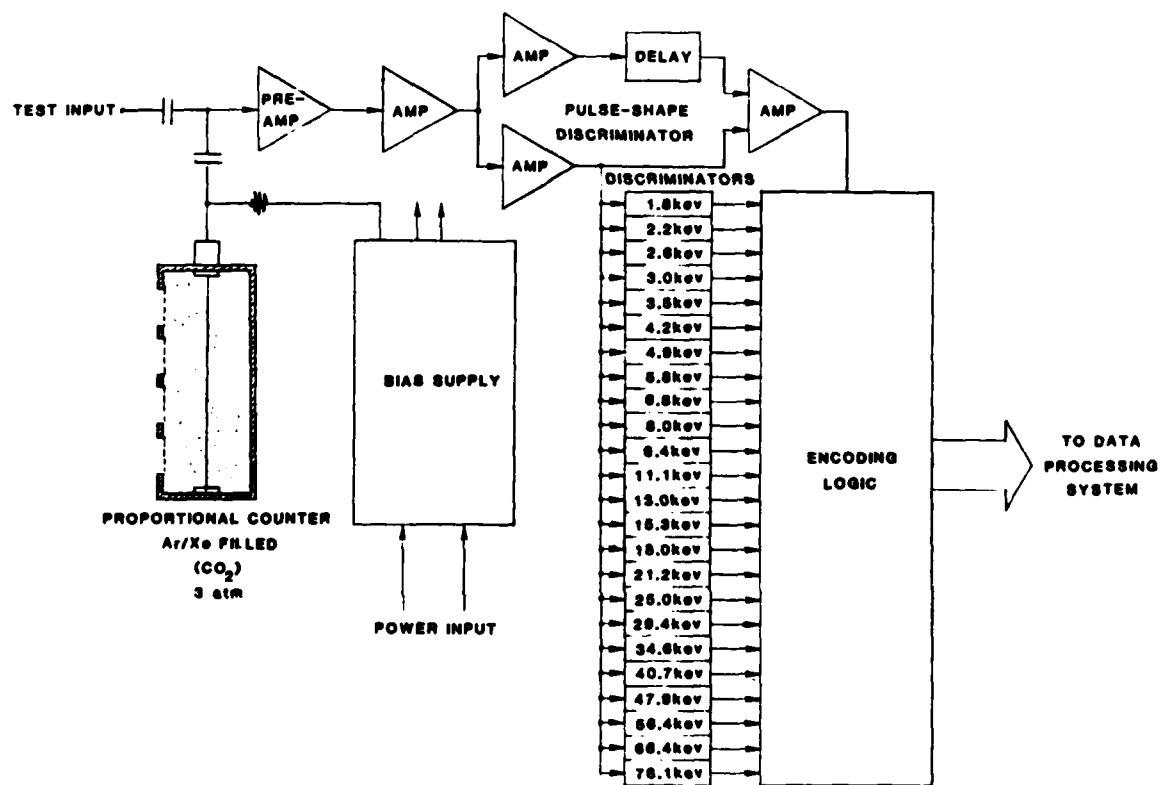


Fig. 5. Block Diagram of the Low-Energy X-Ray Sensor (LEXS)

Energetic charged particles will also cause the PC to produce output signals. However, unlike x rays, these charged particles generate primary ionization tracks that extend over a large portion of the gas-filled region. Charges from the different portions of the track reach the wire at different times, and the resulting output signal has a considerably longer rise time than a signal generated by an x ray. Each signal from the PC is therefore examined by a special rise-time discrimination circuit that produces gating logic pulses corresponding to x rays (X-gate) and to charged particles (E-gate). Within the logic encoding box (see Fig. 5), the X- and E-gate outputs are combined with outputs of PHA discriminators to provide 24 differential x-ray data channels and six charged-particle or background channels. These 30 data outputs, as well as an ungated output of the 1.8-keV discriminator, are encoded into a 5-bit address that is routed to the DPS. Whenever an event aboard the scanner is recorded in one of the data channels, a scaler is identified in the DPS by the transmitted address and updated by a single count. At appropriate times the scalars are read out and the data are merged with the telemetry-data stream.

C. GEIGER-MUELLER BACKGROUND MONITORS (GMBM)

Two monitors of electron flux have been incorporated in the SSB/A. They are Dosimeter Corporation model 6213 Geiger-Mueller counters having $1.4\text{-}\mu\text{gm/cm}^2$ mica windows, with a sufficient thickness of aluminum foil placed in front of the mica window to provide the desired electron-energy detection threshold. The respective energy thresholds of the two counters are approximately 50 and 100 keV. Each tube is part of an independent system consisting of an amplifier, a discriminator, and a bias supply. A block diagram of the system is shown in Fig. 6.

Both sensors are mounted so that their fields of view form 45° half-angle cones centered about the y direction. They will thus detect electrons whose pitch angles are near 90° at high latitudes and which produce local bremsstrahlung by striking the satellite structure.

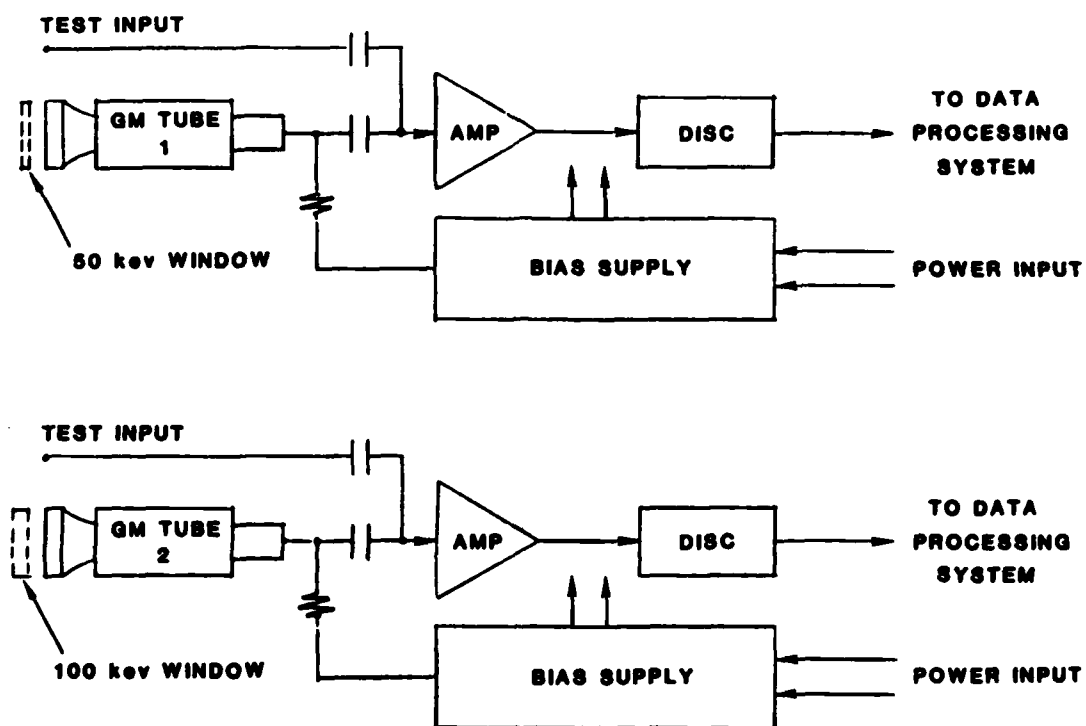


Fig. 6. Block Diagram of the Geiger-Mueller (GM) Sensors

D. HYDROGEN LYMAN-ALPHA RADIATION MONITOR (HLARM)

The HLARM was included in the detector complement to provide a method of detecting the proton aurora, i.e., the atmospheric emissions caused by precipitating protons. One of these emissions is the hydrogen Lyman-alpha line at a wavelength of 1216 Å, whose intensity is measured by the HLARM.

Figure 7 is a functional block diagram of the HLARM, which is a self-contained unit attached to the side of the LEXS scanning head so that the Lyman-alpha and x-ray fluxes enter the two sensors from the same direction and are measured simultaneously. The HLARM sensing element is a channel-electron multiplier (CEM) with a filter placed in front.

The filter consists of a sealed gas-absorption cell containing oxygen at 0.54 atm pressure with a 1% admixture of helium as an aid in leak detection. This particular filter makes use of the fact that oxygen absorbs its own strong emissions at 1304 Å and 1356 Å, as well as at the 1200-Å nitrogen-emission line that the detector would also see. The filter is transparent to the 1216-Å hydrogen-emission line. The cell has a window 1 mm thick of magnesium fluoride and/or a path length in the gas of approximately 7.5 mm. Pressure in the cell is monitored continuously by means of a transducer whose output is sampled by the multiplexed analog-to-digital converter in the DPS. At the entrance to the filter cell, a mechanical collimator defines a rectangular field of view. A full angle of 8° is subtended in the x-y plane (in-track) and 14° in the x-z plane (cross-track).

Light emerging from the filter strikes the channel-electron multiplier (CEM) that is operated in the saturated pulse-counting mode. Pulses at the output are detected and shaped by a discriminator and routed to a scaler in the DPS. The CEM high-voltage bias is measured continuously by a high-voltage monitor whose output is sampled by the DPS-multiplexed analog-to-digital converter. The scaler output as well as the analog-to-digital converter outputs corresponding to the filter pressure and CEM high-voltage values are encoded by the DPS into the digital data stream.

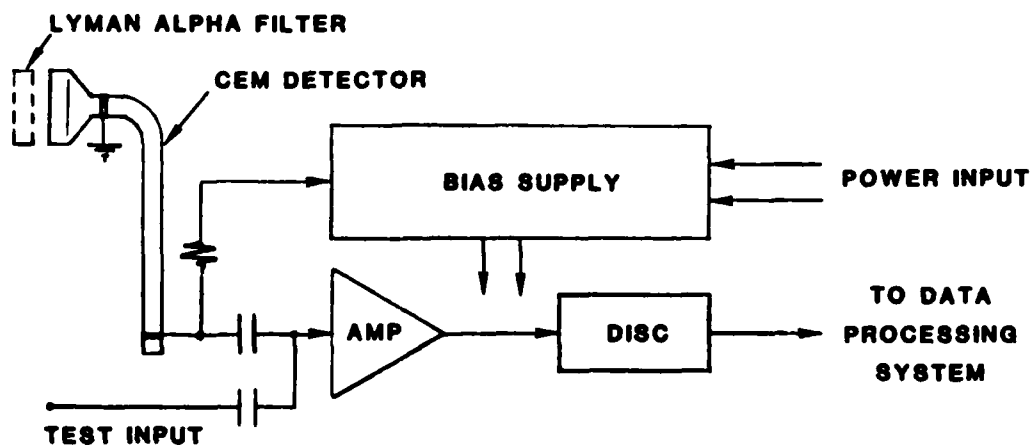


Fig. 7. Block Diagram of the Hydrogen Lyman-Alpha Radiation Monitor (HLARM)

E. SCANNER DRIVE AND CONTROL SYSTEM

Each of the two SSB/A scanning heads is powered by one of two identical, separately powered drivers. The motions of each scanning head are the same, but opposite in the rotational sense. This reduces the level of uncompensated angular momentum disturbance felt by the spacecraft.

In normal operation each head scans in the x-z plane (see Fig. 3). The normal scan limit is reached as the heads move 50.04° from the nadir position towards each other; the direction is reversed and immediately the heads scan to the "outboard" limit, where their fields of view point away from each other. The outboard limit lies 59.22° from the nadir position. Total scan travel is thus 109.26° .

The driver is a Singer Corporation size-8 step motor that is rigidly coupled to an integral gearhead having a reduction ratio of 62.2596:1. The motor and gearhead have been specially prepared for space use.

The motor/gearhead combination couples into a slipclutch through a 2:1 reduction. The slipclutch is necessary to avoid introducing excessive torque loads to the motor gearhead during handling and vibrational excitation. Since high reduction-ratio instrument gear trains will develop torque levels far beyond their capacity, a slipclutch is also needed in the event of momentary overload.

The slipclutch drives the scanner head input shaft through an additional 86/26 reduction. The overall reduction from the step motor output shaft to the scanner input shaft is then $62.2596 \times 2/1 \times 86/26 = 411.87:1$. Therefore, the scanner head moves $90/411.87 = 0.218^\circ$ per step. The self-contained gearbox is coupled to the scanner head through a spline coupling to allow easy assembly and disassembly. The gearheads also contain an antibacklash spring that keeps the scanning heads loaded in one direction at all times, to avoid errors introduced by backlash.

In addition to the reduction train, the gearbox includes a feedback potentiometer that is used to verify the scanner head motion. The potentiometer is coupled to the gearbox output shaft (scanner head input) via a step-up gearmesh of ratio 82/26. The step-up is used to increase the potentiometer resolution. Since the scanner head motion is restricted to a total of 109.26° , the potentiometer does not make a complete revolution and thus does not have any ambiguous positions. The potentiometer rotates $0.218 \times 82/26 = 0.69^\circ$ for each motor step, in a direction opposite to that of the scanner head rotation. Table 2 shows the pointing angle of each head during the middle of each 1-sec data subframe, together with the corresponding potentiometer readings. The angles are positive when the sensors point outboard (away from each other) and negative inboard from the nadir.

In normal operation the end points of scanner-head travel are determined entirely by counting control-system pulses to the step motors. Starting from any random location, the control system initiates a synchronization sequence, following which the scanner heads move first 500 steps in one direction, then 500 steps in the opposite direction. The cycle continues in a totally open-loop fashion, each scanner head being independently slaved to the control-system inputs.

In case a disturbance in the control system causes either scanner head to move beyond its normal turnaround point, a maximum error of 1° may occur before the actuation of a limit switch that initiates a new synchronization sequence. Should the heads be forced to move beyond the limit switch actuation points an additional degree of travel will bring the scanner heads to a firm mechanical stop. It is unlikely this would occur at any time other than during the launch sequence, at which time the scanner heads are not caged.

F. DATA-PROCESSING SYSTEM

The digital flight-data system for the SSB/A provides a serial data-output channel of 684 bits per second. Data from this channel are read out under synchronized control of the spacecraft, which provides the DPS with signals in the form of the special-sensor-read gate and bit-clock pulses.

Table 2. Scanner Pointing Directions

Subframe	Pointing Angle, deg	PC Potentiometer Reading	CT Potentiometer Reading
0	-39.4	3288	376
1	-47.5	3592	88
2	-38.8	3320	360
3	-27.9	2936	728
4	-16.9	2568	1112
5	-6.0	2200	1496
6	+4.9	1832	1864
7	+15.8	1464	2248
8	+26.8	1096	2616
9	+37.7	728	2984
10	+48.6	360	3352
11	+56.8	72	3656
12	+48.0	312	3400
13	+37.0	680	3016
14	+26.1	1048	2648
15	+15.2	1432	2264
16	+4.3	1800	1896
17	-6.7	2184	1512
18	-17.6	2552	1128
19	-28.5	2920	760

In addition to the above readout-control signals, the DPS also accepts from the spacecraft the power-enable signals and the serial command in the form of an 8-bit word. Each of the 8 bits in the serial command has a unique function associated with it; in other words, the 8 bits comprise a set of eight independent switches, each of which controls a specific sensor state. Following receipt of a new serial command, the DPS interprets the 8 bit values, sends appropriate control signals to the SSB/A components, and sets the values of the command-status bits for incorporation into the digital data stream. At the same time, the interpreted bit values are presented to the spacecraft discrete, experiment-status telemetry (DEST) inputs in the form of voltage levels (0 V = "1"; 5 V = "0"). Table 3 lists all the command-status (CS) bits that have been encoded in the data stream and identifies the respective functions associated with these bits. Note that there is a one-to-one correspondence between the serial-command and command-status bits.

In addition to the eight command-status levels, the DEST list includes the CT-head heater on/off status, where 5 V = on and 0 V = off. The spacecraft telemetry also includes four analog experiment-status telemetry (AEST) channels, namely the CT1 detector temperature, the SSB/A base-plate temperature, and the temperatures of the sensor thermal covers (designated as X1 temp and X2 temp). A table for converting AEST voltages to temperature is given in Appendix A.

As mentioned in the description of the individual sensor components, data from the various detectors, in the form of counts, are accumulated in the DPS scalars. There are 52 of these scalars, a number corresponding to the total number of data channels. In order to minimize the amount of hardware needed to provide the required accuracy of data processing, counts from each data channel are accumulated in a 12-bit scaler for 10 msec, then added via a serial adder to the appropriate location in a 1024-bit RAM accumulator during the next 10-msec scaler counting period. After 92 scaler readout cycles, the scalars are disabled, approximately 10 msec before the read-gate pulse arrives. Upon receipt of the read-gate signal, the data are read out from the RAM via a data compressor, merged with digital health-status information, and presented to the spacecraft in the form of 60 bits containing the health-

Table 3. Command Status Table

Bit No.	Subsystem Affected	Bit Value	Status
0	Scanner drive	0	Pointing to nadir,
		1	scanning
1	CT motor power	0	Off
		1	On
2	PC motor power	0	Off
		1	On
3	CT detector bias	0	Off
		1	On
4	PC bias	0	Off
		1	On
5	PM bias	0	Off
		1	On
6	GM detectors	0	Off
		1	On
7	HLARM	0	Off
		1	On

status information plus 52 12-bit binary floating-point words of sensor data, for a total of 684 bits. The complete process described above occurs once per second at the start of each data subframe and lasts 70 msec. After the read-out is complete, the scalers are again enabled. A complete description of the digital data format, with a description of the binary floating-point compression algorithm, is provided in Section 4 of this report.

In terms of actual hardware, the circuitry consists of 9 boards, approximately 14 x 13 cm each, containing a total of about 230 MSI-level integrated circuits. With the exception of nine bipolar components, all of the above are radiation-hardened CMOS devices capable of surviving 10^5 rad (Si). The bipolar devices have a much higher radiation tolerance.

Several features representing a significant advance over the design of previously flown systems (e.g., the GFE-6 sensor) have been incorporated in the SSB/A DPS electronic system in order to save space and mass. Some of these are the following:

- a. New partial-sum scalers (52 channels of 12 bits/10 msec) operated in conjunction with a RAM accumulator.
- b. Serial adder.
- c. 1024-bit RAM accumulator (1-sec input data capacity).
- d. Serial floating-point output-data compressor.
- e. 100-kHz, two-phase clock-driven random logic controller (clock PPL synchronously derived from the 10-kHz reference clock input signal from the OLS).

IV. DATA FORMATS

A brief description of the data processing system hardware and the method used to incorporate the various SSB/A data channels in the serial-bit stream has been provided in Section III. This section contains a more detailed description of the bit-stream format and the various data channels associated with the individual sensor components. Augmented by the background information provided in the other portions of this report, this section is intended to serve as the primary operational reference guide for processing the SSB/A information contained in the spacecraft serial data stream.

A. DATA ORGANIZATION

The various SSB/A data channels can be arranged into four broad categories or groups, according to their origin or function. Table 4 identifies the four groups and the individual channels belonging to each group. In addition, Table 4 shows the location of each SSB/A data channel within the serial-bit stream, with the latter subdivided into 57 12-bit words.

The basic unit of the SSB/A data is the 1-sec subframe, which consists of a block of 684 bits or 57 12-bit words. The latter are numbered according to the convention that bits 0 through 11 of word 1 are the bits transferred first, in that order, to the OLS data stream, followed by bits 0 through 11 of word 2 and so on, until all the 684 bits in the data block are read by the OLS.

Most of the SSB/A data are read out once every second. However, some of the Group 1 diagnostic data channels (see Table 4) are multiplexed for lack of sufficient telemetry space. In particular, temperature, pressure, and bias-monitor data are read out via a 20-sec, 7-bit subcom word. The subframe number, ranging in value from 0 through 19 and corresponding to each subcom measurement, appears in the 5-bit subframe-ID word. Table 5 is a list of the subframe ID values and the corresponding subcom measurements. The tables necessary to convert the digital subcom word values to engineering units are given in Appendixes B and C.

Table 4. SSB/A Data-Channel Organization

Group No.	Channel Designation	T/M Word No.	No. of Bits
1	Diagnostic data	See Table 6	
	Dosimeter	See Table 5	8
	Subframe ID	See Table 5	5
	Subcom	See Table 5	8
	Noise ID	See Table 5	1
	Noise monitor	See Table 5	6
	Command status	See Table 5	8
	PC POT (PCP)	4	12
	CT POT (CTP)	5	12
2	Auxiliary Data		
	GM1	39	12
	GM2	38	12
	LA	37	12
	PM1	52	12
	PM2	46	12
	PM3	40	12
3	CdTe (HEXS)		
	CT1-U	57	12
	CT1-1	56	12
	CT1-2	55	12
	CT1-3	54	12
	CT1-4	53	12
	CT2-U	51	12
	CT2-1	50	12
	CT2-2	49	12
	CT2-3	48	12
	CT2-4	47	12
	CT3-U	45	12
	CT3-1	44	12
	CT3-2	43	12
	CT3-3	42	12
	CT3-4	41	12
4	Proportional counter (LEXS)		
	PCS	21	12
	X1	6	12
	X2	22	12
	X3	7	12
	X4	23	12
	X5	8	12
	X6	24	12

Table 4. SSB/A Data-Channel Organization (Continued)

Group No.	Channel Designation	T/M Word No.	No. of Bits
4	X7	9	12
	X8	25	12
	X9	10	12
	X10	26	12
	X11	11	12
	X12	27	12
	X13	12	12
	X14	28	12
	X15	13	12
	X16	29	12
	X17	14	12
	X18	30	12
	X19	15	12
	X20	31	12
	X21	16	12
	X22	32	12
	X23	17	12
	X24	33	12
	E1	18	12
	E2	34	12
	E3	19	12
	E4	35	12
	E5	20	12
	E6	36	12

Table 5. List of Subcom Measurements

Subframe ID	Measurement
0	CT-1 module-face temperature
1	CT-2 detector temperature
2	CT-3 detector temperature
3	Not used
4	Low-voltage power supply temperature
5	Not used
6	Not used
7	PC face temperature
8	PC high-voltage supply temperature
9	PC electronics temperature
10	+10-V monitor
11	+5-V monitor
12	-5-V monitor
13	PC high-voltage monitor
14	PMT high-voltage monitor
15	HLARM high-voltage monitor
16	HLARM pressure monitor
17	CT-1 noise monitor
18	CT-2 noise monitor
19	CT-3 noise monitor

Noise on the three CT HEXS detectors is read out via a 6-bit, 3-sec subcommutator. The noise monitor samples detector CT1 first, CT2 next, and CT3 last. A single bit, designated as the noise monitor ID, has the value "1" when the noise-monitor data pertain to CT1, and "0" otherwise.

The Group 1 or diagnostic data all occur in the first 5 words or 60 bits of the data subframe. Words 4 and 5 contain pointing information for the scanning PC and CT heads, respectively. They are labeled PC POT and CT POT in Table 4. The values taken on by the pointing indicators and the corresponding angles are listed in Table 2. All of the other diagnostic-data channels are contained in words 1 through 3, in a rather scrambled form. The reasons for this scrambling are historical in nature and irrelevant to the present discussion. Table 6 is an attempt to provide a means of unscrambling the diagnostic data.

Of the Group 1 data words, the subframe ID, subcom, noise ID, noise monitor, PD POT, and CT POT have been discussed above. The dosimeter channel contains data concerning the interpreted, total x-ray intensity flux measured by the LEXS (PC). The discussion of the use and measurement of these data is beyond the scope of this report. The command-status word provides information of the SSB/A operational configuration achieved by sending the serial 8-bit stored command. Table 3 provides the information needed to determine this status from the command status word.

Data contained in all the 12-bit words of Groups 2, 3, and 4 represent counts registered by the various photon and particle detectors described in Section 3. Thus, the Group 2 auxiliary data consist of counts from the two geiger counters (GM1 and GM2), the Lyman-alpha Detector (LA), and the three veto counters in the HEXS. The Group 3 CT (HEXS) data consist of counts in the single, ungated (e.g., CT1-U) and the four gated (e.g., CT2-1, CT2-2, CT2-3, and CT2-4) channels from each of the three CT detectors comprising the HEXS (CT1, CT2, and CT3). Similarly, the Group 4 proportional counter (LEXS) data consist of counts in each of the 24 differential x-ray channels (X1 - X24), the six differential particle channels of the LEXS, and the total counts channel (PCS).

Table 6. Diagnostic Data (Group 1) Organization

Word No.	Bit No.											
	0	1	2	3	4	5	6	7	8	9	10	11
1	A2	A3	A4	A5	A6	A7	B0	B1	B2	B3	B4	C0
2	D1	D2	D3	D4	D5	D6	D7	D0	E0	E1	A0	A1
3	E2	E3	E4	E5	F0	F1	F2	F3	F4	F5	F6	F7

Key:

- A = Dosimeter (8 bits)
- B = Subframe ID (5 bits)
- C = Noise monitor ID (1 bit)
- D = Subcom (8 bits)
- E = Noise monitor (6 bits)
- F = Command status (8 bits)

B. DATA COMPRESSION SCHEME

In the case of the SSB/A data represented by Data Groups 2, 3, and 4, the 12-bit assignment for each data channel is insufficient to prevent occasional overflow in the counts accumulated during 1 sec. Consequently, a special binary floating-point data-encoding scheme was used. By use of this scheme, counting rates of approximately 4×10^5 counts per sec can be accommodated without overflow while the accuracy in the data can be retained better than that associated with counting statistics.

From an operational point of view, the quantity of most interest is the actual number of counts accumulated in each data channel. Hence, rather than dwelling on the logic used to implement the compression scheme, we present below an algorithm to be used in "decompressing" the data, without attempting to derive it.

Before presenting the equations used to decode the compressed data, we define several quantities. First we define the function $\text{INT}(X)$ as the integer portion of the real number X . Thus $\text{INT}(X)$ is the integer obtained by ignoring all digits to the right of the decimal place in X . Letting IC represent the compressed value of any of the relevant 12-bit words, we compute the quantities

$$IN = \text{INT}(IC/256)$$

and

$$M = IC - 256IN$$

We further define the quantity δ according to the prescription

$$\delta = 0 \text{ for words 7 through 20 and 22 through 36}$$

and

$\delta = 1$ for all others

In terms of the above quantities, the value U of the decoded data is given by one of the following two expressions, depending on the value of IC :

Case 1, $IC < 512$:

$$U = (IC - \delta) / 0.92$$

and

Case 2, $IC \geq 512$:

$$U = [(256 + M + 0.5) \times 2^{IN-1} - 0.5 - \delta] / 0.92$$

The factor 0.92 prominent in the expressions above represents a correction for dead time incurred in formatting, compressing, and shifting out the data within the data processing system. Likewise, the quantity δ is used to correct the data for the single count intentionally added to certain channels by the SSB/A hardware.

REFERENCES

1. W. A. Kolasinski and P. F. Mizera, "The GFE-6 Sensor," Aerospace Report No. TR-0077(2632)-1.
2. P. F. Mizera, J. R. Luhmann, W. A. Kolasinski, and J. B. Blake, "Correlated Observations of Auroral Arcs, Electrons, and X Rays from a DMSP Satellite," J. Geophys. Res. 83, 5573 (1978).
3. P. F. Mizera and D. J. Gorney, Private communication.

APPENDIX A. CONVERSION OF THE AEST WORDS FROM ANALOG
(0 - 4.89 V) TO TEMPERATURE IN °C

	0.02	0.03	0.04	0.05	0.06	0.07	0.08	0.09
0.0	-87.9	-82.5	-76.0	-72.7	-70.1	-67.8	-65.9	-64.3
0.1	-81.4	-76.0	-69.5	-67.0	-65.0	-63.1	-61.3	-59.7
0.2	-75.0	-69.5	-63.0	-60.5	-58.5	-56.6	-54.8	-53.2
0.3	-68.6	-63.0	-56.5	-54.0	-52.0	-50.1	-48.3	-46.7
0.4	-62.2	-56.5	-50.0	-47.5	-45.5	-43.6	-41.8	-40.2
0.5	-55.8	-50.0	-43.5	-41.0	-39.0	-37.1	-35.3	-33.7
0.6	-49.4	-43.5	-37.0	-34.5	-32.5	-30.6	-28.8	-27.2
0.7	-43.0	-37.0	-30.5	-28.0	-26.0	-24.1	-22.3	-20.7
0.8	-36.6	-30.5	-24.0	-21.5	-19.5	-17.6	-15.8	-14.2
0.9	-30.2	-24.0	-17.5	-15.0	-13.0	-11.1	-9.3	-7.7
1.0	-23.8	-17.5	-11.0	-8.5	-6.5	-4.6	-2.8	-1.2
1.1	-17.4	-11.0	-4.5	-2.0	0.0	1.9	3.7	5.3
1.2	-11.0	-4.5	2.0	4.5	6.5	8.6	10.8	12.2
1.3	-4.6	2.0	4.5	6.5	8.6	10.8	13.0	14.4
1.4	1.8	4.5	6.5	8.6	10.8	13.0	15.2	16.6
1.5	5.2	6.5	8.6	10.8	13.0	15.2	17.4	18.8
1.6	8.6	10.8	13.0	15.2	17.4	19.6	21.8	23.2
1.7	12.0	13.0	15.2	17.4	19.6	21.8	24.0	25.4
1.8	15.4	17.4	19.6	21.8	24.0	26.2	28.4	29.8
1.9	18.8	21.8	24.0	26.2	28.4	30.6	32.8	34.2
2.0	22.2	24.0	26.2	28.4	30.6	32.8	35.0	36.4
2.1	25.6	27.4	29.6	31.8	34.0	36.2	38.4	39.8
2.2	29.0	30.5	32.5	34.5	36.5	38.5	40.5	41.9
2.3	32.4	33.5	35.5	37.5	39.5	41.5	43.5	44.9
2.4	35.8	36.5	38.5	40.5	42.5	44.5	46.5	47.9
2.5	39.2	39.5	41.5	43.5	45.5	47.5	49.5	50.9
2.6	42.6	42.5	44.5	46.5	48.5	50.5	52.5	53.9
2.7	46.0	45.5	47.5	49.5	51.5	53.5	55.5	56.9
2.8	49.4	48.5	50.5	52.5	54.5	56.5	58.5	59.9
2.9	52.8	51.5	53.5	55.5	57.5	59.5	61.5	62.9
3.0	56.2	54.5	56.5	58.5	60.5	62.5	64.5	65.9
3.1	59.6	57.5	59.5	61.5	63.5	65.5	67.5	68.9
3.2	63.0	60.5	62.5	64.5	66.5	68.5	70.5	71.9
3.3	66.4	63.5	65.5	67.5	69.5	71.5	73.5	74.9
3.4	69.8	66.5	68.5	70.5	72.5	74.5	76.5	77.9
3.5	73.2	69.5	71.5	73.5	75.5	77.5	79.5	80.9
3.6	76.6	72.5	74.5	76.5	78.5	80.5	82.5	83.9
3.7	80.0	75.5	77.5	79.5	81.5	83.5	85.5	86.9
3.8	83.4	78.5	80.5	82.5	84.5	86.5	88.5	89.9
3.9	86.8	81.5	83.5	85.5	87.5	89.5	91.5	92.9
4.0	90.2	84.5	86.5	88.5	90.5	92.5	94.5	95.9
4.1	93.6	87.5	89.5	91.5	93.5	95.5	97.5	98.9
4.2	97.0	90.5	92.5	94.5	96.5	98.5	100.5	101.9
4.3	100.4	93.5	95.5	97.5	99.5	101.5	103.5	104.9
4.4	103.8	96.5	98.5	100.5	102.5	104.5	106.5	107.9
4.5	107.2	100.0	101.5	103.5	105.5	107.5	109.5	110.9
4.6	110.6	103.0	104.5	106.5	108.5	110.5	112.5	113.9
4.7	114.0	106.0	107.5	109.5	111.5	113.5	115.5	116.9
4.8	117.4	109.0	110.5	112.5	114.5	116.5	118.5	119.9

APPENDIX B. CONVERSION OF INTERNAL SUBCOM VALUES FROM
DIGITAL (OCTAL) TO TEMPERATURE IN °C

	0.	1.	2.	3.	4.	5.	6.	7.
00.	-76.7	-66.0	-60.0	-55.7	-52.4	-49.6	-47.2	-45.1
01.	-43.2	-41.4	-39.8	-38.4	-37.0	-35.7	-34.4	-33.2
02.	-32.1	-31.0	-30.0	-29.0	-28.0	-27.1	-26.2	-25.3
03.	-24.4	-23.6	-22.8	-22.0	-21.2	-20.4	-19.7	-18.9
04.	-18.2	-17.4	-16.7	-16.0	-15.3	-14.6	-13.9	-13.3
05.	-12.6	-11.9	-11.3	-10.6	-9.9	-9.3	-8.6	-8.0
06.	-7.3	-6.7	-6.1	-5.4	-4.8	-4.1	-3.5	-2.8
07.	-2.2	-1.6	-0.9	-0.3	0.4	1.0	1.7	2.4
10.	3.0	3.7	4.4	5.1	5.7	6.4	7.1	7.8
11.	8.6	9.3	10.0	10.8	11.5	12.3	13.0	13.8
12.	14.6	15.4	16.3	17.1	18.0	18.9	19.8	20.7
13.	21.6	22.6	23.6	24.6	25.7	26.8	27.9	29.1
14.	30.3	31.6	32.9	34.3	35.7	37.2	38.8	40.5
15.	42.3	44.2	46.3	48.5	50.9	53.6	56.5	59.8
16.	63.5	67.7	72.8	78.9	86.8	97.7		
17.								

APPENDIX C. CONVERSION OF INTERNAL SUBCOM VALUES FROM
DIGITAL (OCTAL) TO VOLTS

	0.	1.	2.	3.	4.	5.	6.	7.
00.	0.028	0.070	0.111	0.153	0.195	0.236	0.278	0.319
01.	0.361	0.402	0.444	0.485	0.527	0.569	0.610	0.652
02.	0.693	0.735	0.776	0.818	0.860	0.901	0.943	0.984
03.	1.026	1.067	1.109	1.150	1.192	1.234	1.275	1.317
04.	1.358	1.400	1.441	1.483	1.525	1.566	1.608	1.649
05.	1.691	1.732	1.774	1.815	1.857	1.899	1.940	1.982
06.	2.023	2.065	2.106	2.148	2.190	2.231	2.273	2.314
07.	2.356	2.397	2.439	2.480	2.522	2.564	2.605	2.647
10.	2.688	2.730	2.771	2.813	2.855	2.896	2.938	2.979
11.	3.021	3.062	3.104	3.145	3.187	3.229	3.270	3.312
12.	3.353	3.395	3.436	3.478	3.520	3.561	3.603	3.644
13.	3.686	3.727	3.769	3.810	3.852	3.894	3.935	3.977
14.	4.018	4.060	4.101	4.143	4.185	4.226	4.268	4.309
15.	4.351	4.392	4.434	4.475	4.517	4.559	4.600	4.642
16.	4.683	4.725	4.766	4.808	4.850	4.891	4.933	4.974
17.								

LABORATORY OPERATIONS

The Laboratory Operations of The Aerospace Corporation is conducting experimental and theoretical investigations necessary for the evaluation and application of scientific advances to new military space systems. Versatility and flexibility have been developed to a high degree by the laboratory personnel in dealing with the many problems encountered in the nation's rapidly developing space systems. Expertise in the latest scientific developments is vital to the accomplishment of tasks related to these problems. The laboratories that contribute to this research are:

Aerophysics Laboratory: Launch vehicle and reentry aerodynamics and heat transfer, propulsion chemistry and fluid mechanics, structural mechanics, flight dynamics; high-temperature thermomechanics, gas kinetics and radiation; research in environmental chemistry and contamination; cw and pulsed chemical laser development including chemical kinetics, spectroscopy, optical resonators and beam pointing, atmospheric propagation, laser effects and countermeasures.

Chemistry and Physics Laboratory: Atmospheric chemical reactions, atmospheric optics, light scattering, state-specific chemical reactions and radiation transport in rocket plumes, applied laser spectroscopy, laser chemistry, battery electrochemistry, space vacuum and radiation effects on materials, lubrication and surface phenomena, thermionic emission, photosensitive materials and detectors, atomic frequency standards, and bioenvironmental research and monitoring.

Electronics Research Laboratory: Microelectronics, GaAs low-noise and power devices, semiconductor lasers, electromagnetic and optical propagation phenomena, quantum electronics, laser communications, lidar, and electro-optics; communication sciences, applied electronics, semiconductor crystal and device physics, radiometric imaging; millimeter-wave and microwave technology.

Information Sciences Research Office: Program verification, program translation, performance-sensitive system design, distributed architectures for spaceborne computers, fault-tolerant computer systems, artificial intelligence, and microelectronics applications.

Materials Sciences Laboratory: Development of new materials: metal matrix composites, polymers, and new forms of carbon; component failure analysis and reliability; fracture mechanics and stress corrosion; evaluation of materials in space environment; materials performance in space transportation systems; analysis of systems vulnerability and survivability in enemy-induced environments.

Space Sciences Laboratory: Atmospheric and ionospheric physics, radiation from the atmosphere, density and composition of the upper atmosphere, aurorae and airglow; magnetospheric physics, cosmic rays, generation and propagation of plasma waves in the magnetosphere; solar physics, infrared astronomy; the effects of nuclear explosions, magnetic storms, and solar activity on the earth's atmosphere, ionosphere, and magnetosphere; the effects of optical, electromagnetic, and particulate radiations in space on space systems.

END

FILMED

3-85

DTIC